The important choice of reference environment in microevolutionary climate response predictions

Rolf Ergon

University of South-Eastern Norway

Abstract

It is well documented that individuals of wild populations can adjust to climate change by means of phenotypic plasticity, but few reports on adaptation by means of genetically based microevolution caused by selection. Disentanglement of these separate effects requires that the environmental zero-point (reference environment) is defined, and this should not be done arbitrarily. The problem is that an error in the environmental zero-point may lead to large errors in predicted microevolution. Together with parameter values, the zero-point can be estimated from environmental, phenotypic and fitness data. A prediction error method for this purpose is described, with the feasibility shown by simulations. As shown in a toy example, an estimated environmental zero-point may have large errors, especially for small populations. This may still be a better choice than use of an initial environmental value in a recorded time series, or the mean value, which is often used. Another alternative may be to use the mean value of a past and stationary stochastic environment, which the population is judged to have been fully adapted to, in the sense that the expected geometric mean fitness was at a global maximum. Exceptions are cases with constant phenotypic plasticity, where the microevolutionary changes per generation follow directly from phenotypic and environmental data, independent of the chosen environmental zero-point.

Keywords: Climate response predictions; Environmental zero-point; Microevolution; Plasticity; Prediction error minimization

1 Introduction

Wild populations respond to changing environments by means of phenotypic plasticity and microevolution, and especially climate change responses have been extensively studied. The aim is then to disentangle phenotypic changes owing to genetically based microevolution, caused by natural selection, and changes due to individual phenotypic plasticity. Relying on 11 review articles, including reviews of altogether 66 field studies, Merilä & Hendry (2014) arrived at the conclusion that evidence for genetic adaptation to climate change has been found in some systems, but that such evidence is relatively scarce. They also concluded that more studies were needed, and that these must employ better inferential methods. The aim of the present article is to give a contribution in that respect.

It is obvious that for all evolutionary systems with interval-scaled environmental variables u_t, as for example temperature in ℃, a suitable zero-point (reference environment) u_{ref} must be chosen, and as argued in Section 2 this should not be done arbitrarily. A zero-point is in general defined as "the point on a scale that denotes zero and from which positive and negative readings can be made" (Collins English Dictionary). The problem is that an error in the environmental zero-point may lead to large errors in predicted microevolution. In most cases where the environmental variable is for example a temperature, the zero-point should not, for example, be set to 0 ℃. Neither should it without further consideration be set to the initial or mean environmental value of a specific time series. It appears that the need for a proper environmental zero-point definition, and thus an environmental cue definition, has been largely ignored in the reviewed studies referred to in Merilä & Hendry (2014).

The present article is an attempt to clarify some important questions relating to environmental zero-points, and for that purpose a method for model-based predictions of microevolutionary changes is also proposed. This method is based on parameter estimation by

means of prediction error minimization, including estimation of the environmental zero-point and initial mean values of quantitative traits.

For a discussion of the general microevolution vs. plasticity disentanglement problem, we may for simplicity assume the intercept-slope individual reaction norm model

$$y_{i,t} = a_{i,t} + v_{i,t} + (b_{i,t} + \eta_{i,t})\left(u_t - u_{ref}\right), \tag{1}$$

where $u_t - u_{ref}$ and $y_{i,t}$ are the environmental cue and the individual phenotypic value, respectively, as functions of time t measured in generations. Here, the traits $a_{i,t}$ and $b_{i,t}$ are the additive genetic components of the individual reaction norm intercept and plasticity slope, respectively, while $v_{i,t}$ and $\eta_{i,t}$ are independent iid zero mean normal non-additive effects. The generations are assumed to be non-overlapping.

From Equation (1) follows the mean trait reaction norm model $\bar{y}_t = \bar{a}_t + \bar{b}_t\left(u_t - u_{ref}\right)$, and from this simple equation follows the basic questions discussed in this article. How can the evolution of $\bar{a}_t$ and $\bar{b}_t$ be predicted, provided that u_t and $y_{i,t}$ are known? And how will these predictions be affected by errors in the estimated or assumed value $\hat{u}_{ref}$? It turns out that in order to answer these questions we also need information on individual fitness values $W_{i,t}$.

The environmental zero-point u_{ref} is determined by the environment at which the phenotypic variance has its minimum, as defined in more detail in Section 2, and as discussed in Ergon & Ergon (2017) and Ergon (2018). In theoretical work it is often assumed that the population has fully adapted to a stationary stochastic environment with a given mean value, such that the expected geometric mean fitness is at a global maximum, and the environmental zero-point is then set to zero (Lande, 2009; Chevin & Lande, 2015). Although there is nothing wrong with this theoretical approach, it disguises the underlying problem discussed here, and u_{ref} is therefore included in Equation (1). This formulation also makes it possible to

distinguish between the environment as such, and the environmental cue. In some cases, it may be possible to determine the environmental zero-point experimentally, see, e.g., Fossen *et al*. (2018), but that may obviously be difficult for wild populations.

When the environmental cue $u_t - u_{ref}$ changes over time, the mean trait values $\bar{a}_t$ and $\bar{b}_t$ as follow from Equation (1) may evolve due to selection, and as a result also the mean phenotypic value $\bar{y}_t$ will evolve (Lande, 2009). Without changes due to selection, i.e., if the mean trait values $\bar{a}_t$ and $\bar{b}_t$ are constant, the value of $\bar{y}_t$ may still change when $u_t - u_{ref}$ changes, as also follows from Equation (1).

Section 2 discusses several aspects of the general microevolution vs. plasticity disentanglement problem. First, a definition of the environmental zero-point u_{ref} is given. Second, it is shown how the mean trait values $\bar{a}_t$ and $\bar{b}_t$, and thus also $\bar{y}_t$, evolve as functions of the environmental cue $u_t - u_{ref}$ and the phenotypic selection gradient $\beta_{y,t}$. Third, it is shown how u_{ref} and $\beta_{y,t}$, as well as initial mean trait values and the parameter values in the $\boldsymbol{G}$ matrix, can be estimated by means of a prediction error minimization method (Ljung, 2002), using data from known time series of u_t and $y_{i,t}$, as well as of individual fitness values $W_{i,t}$. Forth, it is discussed why it may be difficult to estimate u_{ref}, as revealed by simulations, and which consequences errors in estimated values of u_{ref} will have. Exceptions are here cases with constant phenotypic plasticity, where the microevolutionary changes per generation follow directly from phenotypic and environmental data, independent of the chosen environmental zero-point.

It must be underlined that the theory in Section 2 assumes that the phenotypic trait $y_{i,t}$ in Equation (1) is not correlated with other phenotypic traits having causal effects on fitness, see Morrissey *et al*. (2010) for a discussion. Also note that the need for a proper environmental zero-point is not specific for the simple case according to Equation (1).

Simulations in Section 3 make use of a toy example, utilizing the intercept-slope reaction norm model in Equation (1). The environmental input u_t is here a noisy positive trend in spring temperature, while the individual phenotypic values $y_{i,t}$ are clutch-initiation date for a certain bird species. The toy example also assumes that the individual fitness values $W_{i,t}$ are the number of offspring. The essential questions are how microevolutionary changes in mean intercept and plasticity slope can be predicted, and how these predictions are affected by errors in the environmental zero-point u_{ref} in Equation (1). The simulations show that errors in the estimated or assumed value of u_{ref} may cause large mean trait prediction errors. They also show the feasibility of the proposed parameter estimation method.

Finally follows a discussion in Section 4. Derivations of prediction equations, simulation results with modeling error and increased population size, and a short comparison with REML parameter estimation are given in Appendix 1 to 4.

2 Theory and methods

2.1 Example system

For a study of the general environmental zero-point problem, and for a test of the proposed parameter estimation method, we may consider a true evolutionary system based on Equation (1),

$$\bar{y}_t = \bar{a}_t + \bar{b}_t\left(u_t - u_{ref}\right), \tag{2a}$$

$$\begin{bmatrix} \Delta\bar{a}_t \\ \Delta\bar{b}_t \end{bmatrix} = \frac{1}{\bar{W}_t}\boldsymbol{GP}^{-1}\begin{bmatrix} cov\left(W_{i,t}, a_{i,t} + v_{i,t}\right) \\ cov\left(W_{i,t}, b_{i,t} + \eta_{i,t}\right) \end{bmatrix}, \tag{2b}$$

with the additive genetic covariance matrix $\boldsymbol{G} = \begin{bmatrix} G_{aa} & G_{ab} \\ G_{ab} & G_{bb} \end{bmatrix}$, and the phenotypic covariance matrix and $\boldsymbol{P} = \begin{bmatrix} G_{aa} + \sigma_v^2 & G_{ab} \\ G_{ab} & G_{bb} + \sigma_\eta^2 \end{bmatrix}$. Here, Equation (2b) is the multivariate breeder's

equation (Lande, 1979), where $W_{i,t}$ is found from any given fitness function. It is assumed that the phenotypic trait $y_{i,t}$ in Equation (1) is not correlated with other phenotypic traits having causal effects on fitness, and that generations are non-overlapping.

2.2 Environmental zero-point

As discussed in the Introduction, there is a need for a well-defined environmental zero-point:

Definition 1

Assuming a single environmental variable u_t, and given a reaction norm model, the environmental zero-point is

$$u_{ref} = u_0 + f(reaction\ norm\ parameter\ values), \tag{3}$$

where u_0 is the environment at which the phenotypic variance is at a minimum, and where the covariance between the plastic phenotypic value and reaction norm slope is zero. Here, $f(reaction\ norm\ parameter\ values)$ is a correction term that may be zero.

For the reaction norm model (1) we find for example (using $u' = u - u_{ref}$)

$$cov(y,b) = E\left[\left(a - \bar{a} + v + \left(b - \bar{b}\right)u' + \eta u'\right)\left(b - \bar{b} + \eta\right)\right] = G_{ab} + \left(G_{bb} + \sigma_\eta^2\right)u', \tag{4a}$$

which by setting $cov(y,b) = 0$ and $u' = u_0 - u_{ref}$ gives the environmental zero-point

$$u_{ref} = u_0 + \frac{G_{ab}}{G_{bb} + \sigma_\eta^2}. \tag{4b}$$

For $G_{ab} = 0$ the environmental zero-point is thus the environment where the phenotypic variance is minimized (see Fig. 1 for illustration). This is also the environment where the expected geometric mean fitness has a global maximum, and thus the environment the population is fully adapted to. In this environment the environmental cue will be zero.

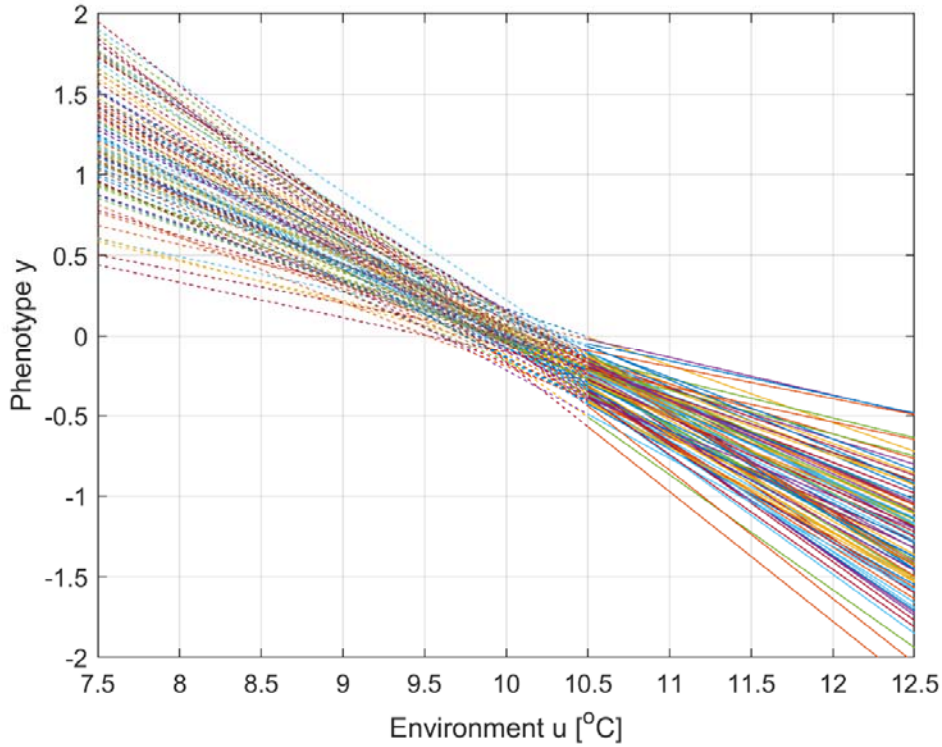

Fig. 1 Reaction norms for 100 individuals in a population according to Equation (1), with $G_{aa} + \sigma_v^2 = 0.05$, $G_{bb} + \sigma_\eta^2 = 0.02$ and $G_{ab} = 0$. The environmental zero-point is $u_{ref} = 10$ °C, which since $G_{ab} = 0$ also is the temperature u_0 to which the population is fully adapted. The mean trait values are $\bar{a}_t = 0$ and $\bar{b}_t = -0.5$. Solid lines indicate the range of data used for parameter estimation and mean trait predictions in simulations. Note that $u_{ref} = u_0 = 10$ °C is not within that range.

2.3 Mean trait prediction equations

A fundamental equation for mean trait predictions follows from Equation (2a) as

$$\Delta\bar{y}_t = \Delta\bar{a}_t + \Delta\bar{b}_t\left(u_{t+1} - u_{ref}\right) + \bar{b}_t \Delta u_t, \tag{5}$$

where $\Delta u_t = u_{t+1} - u_t$, $\Delta\bar{a}_t = \bar{a}_{t+1} - \bar{a}_t$, $\Delta\bar{b}_t = \bar{b}_{t+1} - \bar{b}_t$ and $\Delta\bar{y}_t = \bar{y}_{t+1} - \bar{y}_t$ are changes per generation. From this follows that the value of u_{ref} has nothing to say in special cases

with constant phenotypic plasticity slopes, i.e., when $\Delta\bar{b}_t = 0$. In such cases we simply have $\Delta\bar{y}_t = \Delta\bar{a}_t + \bar{b}\Delta u_t$, where $\bar{b}$ is constant, or only $\Delta\bar{y}_t = \bar{b}\Delta u_t$ if $\bar{a}_t$ does not evolve.

As shown in Appendix 1, Equation (5) leads to equations for $\Delta\bar{a}_t$ and $\Delta\bar{b}_t$ as functions of the phenotypic selection gradient $\beta_{y,t}$,

$$\Delta\bar{a}_t = \left(G_{aa} + G_{ab}\left(u_t - u_{ref}\right)\right)\beta_{y,t} \tag{6a}$$

and

$$\Delta\bar{b}_t = \left(G_{ab} + G_{bb}\left(u_t - u_{ref}\right)\right)\beta_{y,t}, \tag{6b}$$

where

$$\beta_{y,t} = \frac{1}{\bar{W}_t}\left(P_{aa} + 2G_{ab}\left(u_t - u_{ref}\right) + P_{bb}\left(u_t - u_{ref}\right)^2\right)^{-1} cov\left(W_{i,t}, y_{i,t}\right). \tag{6c}$$

In addition to time series of u_t and $y_{i,t}$, we thus need parameter values for u_{ref}, G_{aa}, G_{ab}, G_{bb}, σ_ν^2 and σ_η^2, and a time series of individual fitness values $W_{i,t}$. For mean trait predictions we also need initial values. Note that these equations are valid only when the genetic relationship matrix is a unity matrix (Ch. 26, Lynch & Walsh, 1998).

2.4 Prediction error minimization method

From predicted mean intercept and plasticity slope values found by Equations (6a,b) follows predicted values of $\bar{y}_t$ from Equation (2a). The prediction equations can thus be used for parameter estimation in a prediction error minimization method (PEM), as shown in Fig. 2. As follows from Equations (6a,b,c), we can then set G_{aa} to any value, and estimate G_{ab}, G_{bb}, σ_ν^2 and σ_η^2 relative to that value.

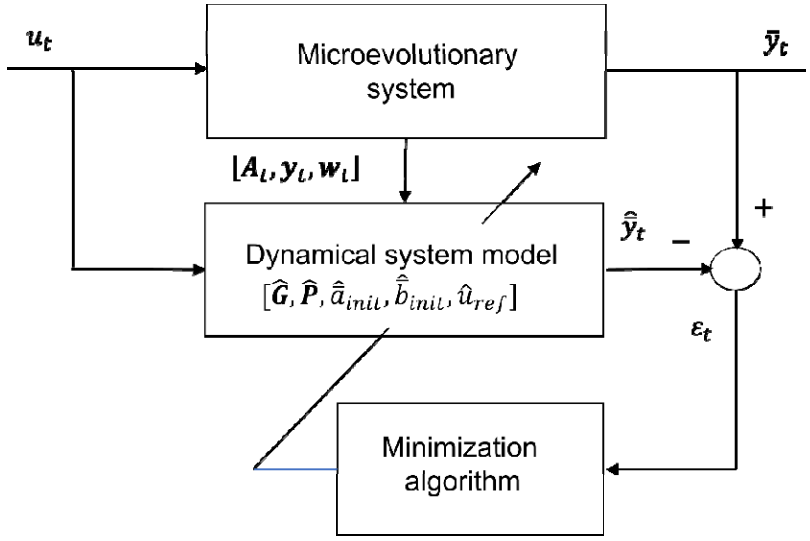

Figure 2. Block diagram of microevolutionary PEM, with dynamical tuning model based on a reaction norm model with mean traits and . Here, and are the known environmental input and the known mean phenotypic value at time , respectively. is the additive genetic relationship matrix, which here is assumed to be , while and are vectors of individual phenotypic and relative fitness values, respectively. The and matrices include the system parameters, while , and are the initial mean trait values and the environmental zero-point, respectively. Assuming data over generations, all these model parameters are tuned until is minimized, with and .

2.5 Effects of environmental zero-point errors

With an environmental zero-point $\hat{u}_{ref}$ instead of u_{ref}, predictions based on Equation (2a) can be written

$$\hat{\bar{y}}_t = \hat{\bar{a}}_t + \hat{\bar{b}}_t\left(u_t - \hat{u}_{ref}\right) = \hat{\bar{a}}_t - \hat{\bar{b}}_t(\hat{u}_{ref} - u_{ref}) + \hat{\bar{b}}_t\left(u_t - u_{ref}\right), \tag{7}$$

where $\hat{\bar{a}}_t$ and $\hat{\bar{b}}_t$ are found from Equations (6a,b) with use of estimated parameter values.

For small values of G_{bb}, i.e., when $G_{bb} \to 0$ and $G_{ab} \to 0$, it follows from Equations (6a,b,c) that $\Delta\bar{a}_t$ is independent of u_{ref}, and that $\bar{b}_t$ is constant. This results in $\Delta\hat{\bar{a}}_t = G_{aa}/(G_{aa} + \hat{\sigma}_v^2)$, such that only $\hat{\sigma}_v^2$ must be tuned in order to minimize $\sum_{t=1}^{T}(\bar{y}_t - \hat{\bar{y}}_t)^2$. In this case an error in $\hat{u}_{ref}$ has very little effect on the change in $\hat{\bar{a}}_t$ over many generations, as also follows from Equation (5).

For larger values of G_{bb} and G_{ab}, $\Delta\hat{\bar{a}}_t$ will be affected by an error in $\hat{u}_{ref}$, and good predictions $\hat{\bar{y}}_t \approx \bar{y}_t$ for $t = 1$ to T can then only be obtained by parameter tuning such that $\hat{\bar{b}}_t \approx \bar{b}_t$ over all generations. That is possible because u_{ref} appears in both nominator and denominator of eqn (6b). According to Equation (7) we then find $\hat{\bar{a}}_t \approx \bar{a}_t + \hat{\bar{b}}_t(\hat{u}_{ref} - u_{ref})$, which as shown in Section 3 may result in large errors in predicted changes of $\bar{a}_t$ over time.

2.6 Effects of modeling errors

Modeling errors will obviously affect predictions of the mean traits. As an example, simulations with the true individual model

$$y_{i,t} = a_{i,t} + v_{i,t} + (b_{i,t} + \eta_{i,t})\left(u_t - c_{i,t} - \gamma_{i,t}\right), \tag{8}$$

are included in Appendix 2. Here, $c_{i,t}$ is a perception trait, as discussed in Ergon & Ergon (2017).

3 Simulation results

3.1 Description of toy example

In the toy example, the environmental input (u_t) is a noisy positive trend in spring temperature, resulting in a noisy negative trend in mean clutch-initiation date ($\bar{y}_t$) for a certain bird species, approximately as in Fig. 2 in Bowers et al. (2016). The individual phenotypic values are discrete, with days as unit. The individual fitness values ($W_{i,t}$) are integers from 0 to 10, with number of fledglings as unit. Generations are assumed to be non-overlapping, and the population size is assumed to be constant. Data for u_t, $y_{i,t}$ and $W_{i,t}$ are generated over 60 generations, where the positive temperature trend begins at generation 10. The population is assumed to be fully adapted to the mean spring temperature 10 °C before generation 10, which is thus the reference environment u_{ref}, but only data from generations 31 to 60 are used for parameter estimation and mean trait predictions. Note that 10 °C may not be within the range of input data used for parameter estimation (depending on realization). The essential questions are how microevolutionary changes in mean intercept and plasticity slope over generations 31 to 60 can be predicted, and how errors in the estimated or assumed value of u_{ref} will affect these predictions.

3.1 True model, fitness function, and environmental input signals

Assume that what we consider to be true mean responses, $\bar{y}_t$, $\bar{a}_t$ and $\bar{b}_t$, are generated by the state-space model (2a,b). Here, $G_{ab} = 0$ in the true system but left as a free parameter in the tuning model in Fig. 2. The individual effects $a_{i,t}$, $b_{i,t}$, $v_{i,t}$ and $\eta_{i,t}$ are at each generation drawn from populations with normal distributions around $\bar{a}_t$, $\bar{b}_t$, 0 and 0, respectively.

The individual fitness function is assumed to be rounded values of

$$W_{i,t} = 10 \cdot exp\left(-\left(y_{i,t} - \theta_t\right)^2 / 2\omega^2\right), \tag{9}$$

where θ_t is the phenotypic value that maximizes fitness, while $\omega^2 = 10$. The discrete values of $W_{i,t}$ (number of fledglings) are thus integers from 0 to 10.

Also assume a stationary or slowly varying mean $\mu_{U,t}$ of a stochastic environment, with added iid zero mean normal random variations $u_{n,t}$ with variance $\sigma^2_{U_n}$, i.e., $u_\mathrm{t} = \mu_{U,t} + u_{n,t}$, and that the population is fully adapted to a stationary stochastic environment with $\mu_{U,t} = u_{ref} = u_0 = 10$ °C (as in Fig. 1). In a corresponding way assume that $\theta_t = \mu_{\Theta,t} + \theta_{n,t}$, where $\theta_{n,t}$ is iid zero mean normal with variance $\sigma^2_{\Theta_n}$, and where $u_{n,t}$ and $\theta_{n,t}$ are correlated with covariance $\sigma_{\Theta_n U_n}$. Following Lande (2009), we may assume that juvenile birds of generation t are exposed to the environment $u_{t-\tau}$ during a critical period of development a fraction of a generation before the adult phenotype is expressed and subjected to natural selection. We will define $\theta_t = -2(u_t - 10)$, which implies a linear relationship $\mu_{\Theta,t} = -2(\mu_{U,t} - 10)$, variances $\sigma^2_{\Theta_n} = 4\sigma^2_{U_n}$, and covariance $\sigma_{\Theta_n U_n} = -2\rho_\tau \sigma^2_{U_n}$, where ρ_τ is the autocorrelation of background environmental fluctuations. We will assume $\sigma^2_{U_n} = 0.5$ and $\rho_\tau = 0.25$. The optimal value of the mean plasticity slope in a stationary stochastic environment is then $\bar{b}_{opt} = \sigma_{\Theta_n U_n}/\sigma^2_{U_n} = -2\rho_\tau = -0.5$ (as in Fig. 1) (Ergon & Ergon, 2017).

Further assume that u_t and θ_t are noisy ramp functions as shown in Fig. 3, with the ramp in $\mu_{U,t}$ starting from 10 °C at $t = 10$ generations. The choice of a negative trend in θ_t, and thus in $\bar{y}_t$, results in earlier clutch-initiation dates as a result of the positive temperature trend.

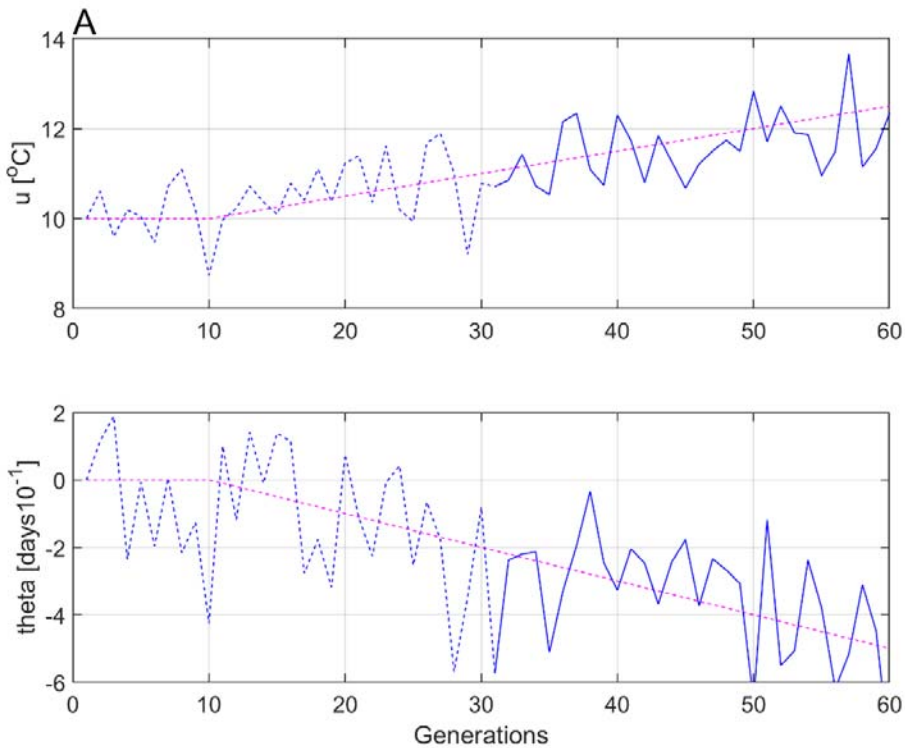

Figure 3. Noisy ramp functions u_t (panel A) and θ_t (panel B), with $u_{ref} = 10$, $\mu_{\Theta,t} = -2(\mu_{U,t} - 10)$, $\sigma^2_{\mathrm{U}_n} = 0.5$, $\sigma^2_{\Theta_n} = 2$ and $\sigma_{\mathrm{U}_n,\Theta_n} = -0.25$. The solid parts of the curves indicate data used for parameter estimation and mean trait predictions (compare with Fig. 1, where reaction norms for $u_t > 10.5$ are indicated by solid lines).

Fig. 4 shows typical individual phenotypic (clutch-initiation date) and fitness (number of fledglings) values for the true model with population size $N = 100$ at generation 45 in Fig. 3. The figure shows that the most negative (earliest) dates give the highest number of offspring, and the population is thus under directional selection towards earlier clutch-initiation dates. The zero date is the mean clutch-initiation date before the positive temperature trend sets in at generation 10 in Fig. 3, when the population is assumed to be under stabilizing selection and fully adapted to the stationary stochastic temperature.

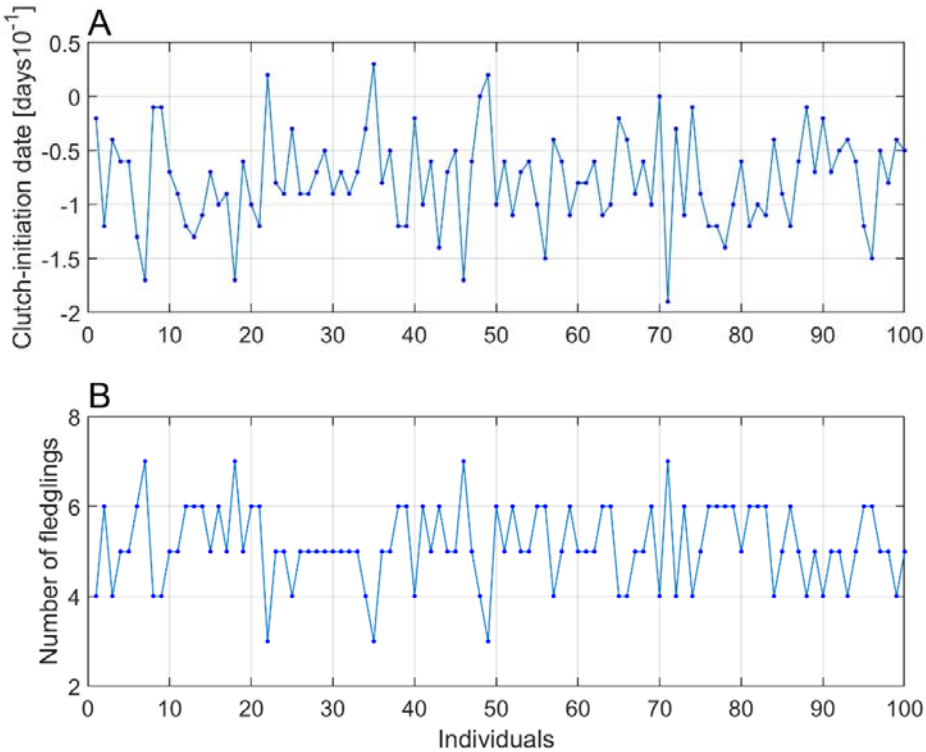

Figure 4. Individual clutch-initiation dates $y_{i,t}$, with a range from -19 to 3 days (phenotypic values, Panel A), and number of fledglings $W_{i,t}$ (fitness, Panel B), at a generation where the population is under directional selection towards earlier clutch-initiation dates. As indicated by dots the number of offspring are integers, while the phenotypic values are integers divided by ten (i.e., days).

3.2 Parameter estimation and mean trait prediction results

Parameter estimation and mean trait prediction results were found by use of the MATLAB function *fmincon* in the PEM method in Fig. 2. Results with use of input-output data from $t = 31$ to 60 with population size $N = 100$ are given in Table 1. The relative errors in total change of predictions over 30 generations are included, computed as $\Delta_{30}^{error}\hat{\bar{a}}_t\% = 100(\Delta_{30}\hat{\bar{a}}_t - \Delta_{30}\bar{a}_t)/\Delta_{30}\bar{a}_t$ etc., where $\Delta_{30}\hat{\bar{a}}_t = \hat{\bar{a}}_{60} - \hat{\bar{a}}_{31}$ and $\Delta_{30}\bar{a}_t = \bar{a}_{60} - \bar{a}_{31}$. The final values $\sum\varepsilon_{t,final}^2$ of $\sum_{t=31}^{60}(\bar{y}_t - \hat{\bar{y}}_t)^2$ are also included, as they indicate the degree of optimization success. Results are presented as mean values and

standard errors, $Mean \pm SE$, based on 100 repeated simulations with different realizations of random inputs.

Given the model in Equations (2a,b) and (9), there are six parameter values to be estimated (while $\hat{\bar{a}}_{31}$ follows from Equation (2a) with $\hat{\bar{y}}_{31}$ sat to zero). In the optimizations the initial values of $\hat{G}_{bb}$, $\hat{G}_{ab}$, $\hat{\sigma}_{\nu}^2$, $\hat{\sigma}_{\eta}^2$ and $\hat{\bar{b}}_{31}$ were set to zero, while the initial value of $\hat{u}_{ref}$ was set to 10 (when $\hat{u}_{ref}$ was a free variable). The true value $\hat{G}_{aa} = 0.025$ was used, such that estimates of G_{bb}, G_{ab}, σ_{ν}^2 and σ_{η}^2 are found relative to $G_{aa} = 0.025$. Table 1 presents results for three cases, first for $\hat{u}_{ref} = u_{ref} = 10$ (Case 1), second for $\hat{u}_{ref}$ as free variable (Case 2), and third for $\hat{u}_{ref} = 11$ (Case 3), which is the expected initial value in the time series used. The estimates of σ_{ν}^2 and σ_{η}^2 have in all cases rather large standard errors, and in some cases also large bias errors. What is more interesting is that the prediction errors $\Delta_{30}^{error}\hat{\bar{a}}_t\%$ and $\Delta_{30}^{error}\hat{\bar{b}}_t\%$ are small in Case 1 (with the correct value $\hat{u}_{ref} = 10$). In Case 2 (with $\hat{u}_{ref}$ as a free variable), $\Delta_{30}^{error}\hat{\bar{a}}_t\%$ has a large standard error. With $\hat{u}_{ref} = 11$ (Case 3), $\Delta_{30}^{error}\hat{\bar{a}}_t\%$ has a large bias error. In this case also the estimates of G_{bb}, G_{ab} and σ_{η}^2 are clearly biased. In all cases $\Delta_{30}^{error}\hat{\bar{b}}_t\%$ is close to the result with the correct value $\hat{u}_{ref} = 10$ (Case 1), as explained in Subsection 2.5.

Table 1 includes theoretical prediction error results based on Equation (7), $\hat{\bar{a}}_{t,corr} = \hat{\bar{a}}_t - \hat{\bar{b}}_t(\hat{u}_{ref} - u_{ref})$. These are in all cases close to the results with $\hat{u}_{ref} = u_{ref} = 10$ (Case 1).

The results for Case 1 and Case 2 are very much improved with population size $N = 10{,}000$, while the standard errors in Case 3 were only marginally improved by an increased population size (Appendix 3). The results for $\hat{u}_{ref}$ in Case 2 were for example improved from 9.92 ± 0.66 to 9.95 ± 0.19 (ideally 10).

Table 1. Estimation and prediction results with true system responses generated by means of Equations (2a,b) and (9). Results are for cases with population size $N = 100$ and perfect observations of $y_{i,t}$ and $W_{i,t}$, and they are based on 100 simulations with different realizations of all random input variables.

Case 1: $\hat{u}_{ref} = 10$ (the true value).

Case 2: $\hat{u}_{ref}$ as a free variable.

Case 3: $\hat{u}_{ref} = 11$ (expected initial value in optimization data). Here, 9% of the simulations were discarded because $\sum \varepsilon_{t,final}^2 > 0.001$.

Parameter etc.	True value	Optimization results Case 1	Optimization results Case 2	Optimization results Case 3
$\hat{G}_{bb}$	0.01	0.0103 ± 0.0023	0.0099 ± 0.0054	0.0065 ± 0.0023
$\hat{G}_{ab}$	0	0.0033 ± 0.0141	0.0028 ± 0.0152	0.0067 ± 0.0022
$\hat{\sigma}_v^2$	0.025	0.0341 ± 0.0141	0.0301 ± 0.0348	0.0264 ± 0.0040
$\hat{\sigma}_\eta^2$	0.01	0.0118 ± 0.0091	0.0123 ± 0.0115	0.0157 ± 0.0037
$\hat{\bar{b}}_{31}$	–	-0.4965 ± 0.0086	-0.4969 ± 0.0083	-0.4985 ± 0.0080
$\hat{u}_{ref}$	10	10	9.9210 ± 0.6553	11
$\sum \varepsilon_{t,final}^2$	–	$10^{-5}(23 \pm 10)$	$10^{-5}(23 \pm 10)$	$10^{-5}(29 \pm 11)$
$\Delta_{30}^{error} \hat{\bar{a}}_t \%$	–	1 ± 4	-5 ± 42	68 ± 8
$\Delta_{30}^{error} \hat{\bar{b}}_t \%$	–	-1 ± 3	0 ± 3	-4 ± 4
$\Delta_{30,corr}^{error} \hat{\bar{a}}_t \%$	–	1 ± 4	0 ± 5	-4 ± 5

As shown in Table 1, a large error in the assumed environmental zero-point $\hat{u}_{ref}$ results in large errors in predicted changes of in $\bar{a}_t$ over 30 generations (Case 3). Table 2 shows prediction results for more moderate errors in $\hat{u}_{ref}$, as well as for $\hat{u}_{ref} = 11.75$ (expected mean value in optimization data), and they are all in accordance with Equation (7).

Table 2. Errors in predicted total relative change of $\bar{a}_t$ and $\bar{b}_t$ over 30 generations, as functions of the environmental zero-point $\hat{u}_{ref}$ used in the optimization procedure.

$\hat{u}_{ref}$	$\Delta_{30}^{error}\hat{\bar{a}}_t\%$	$\Delta_{30}^{error}\hat{\bar{b}}_t\%$
9.75	-16 ± 4	0 ± 3
10	1 ± 4	-1 ± 3
10.25	17 ± 4	0 ± 3
10.5	34 ± 6	-2 ± 3
11	68 ± 8	-4 ± 4
11.75	115 ± 14	-8 ± 6

Fig. 5 shows predicted mean values $\hat{\bar{y}}_t$, $\hat{\bar{a}}_t$ and $\hat{\bar{b}}_t$, as compared to true mean values $\bar{y}_t$, $\bar{a}_t$ and $\bar{b}_t$, for Case 1 and Case 3 in Table 1.

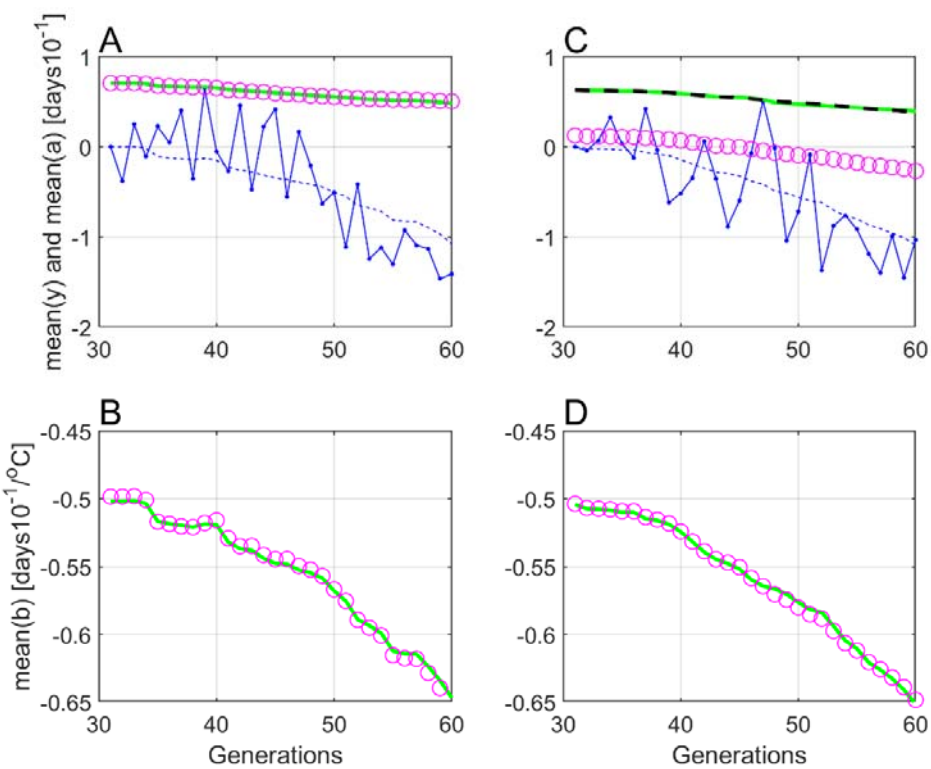

Figure 5. Typical responses for Case 1 and Case 3 in Table 1. True $\bar{y}_t$ values are shown by solid blue lines. All parameter values except $\hat{G}_{aa} = 0.025$ were initially set to zero, which gave predictions $\hat{\bar{y}}_{t,start} = cov(W_{i,t}, y_{i,t})/\bar{W}_t$ as shown by dashed blue lines. Final predictions $\hat{\bar{y}}_t$ are shown by blue dots. True $\bar{a}_t$ and $\bar{b}_t$ responses are shown by green lines, while predictions $\hat{\bar{a}}_t$ and $\hat{\bar{b}}_t$ are shown by magenta circles. Panels A and B show results for Case 1 with $\hat{u}_{ref} = 10$ (true value), while panels C and D show results for Case 3 with $\hat{u}_{ref} = 11$. Here, the theoretical predictions $\hat{\bar{a}}_{t,corr} = \hat{\bar{a}}_t - \hat{\bar{b}}_t(\hat{u}_{ref} - u_{ref})$ are included as black dashed line. Note that $\bar{y}_{31} = \hat{\bar{y}}_{31}$ is set to zero, such that $\bar{a}_{31} = -\bar{b}_{31}(u_{31} - 10)$ and $\hat{\bar{a}}_{31} = -\hat{\bar{b}}_{31}(u_{31} - \hat{u}_{ref})$, where u_{31} is not quite the same from realization to realization.

4 Discussion

It is well documented that populations adjust to climate change by means of individual plasticity, but few reports on adaptation by means of genetically based microevolution caused by phenotypic selection (Merilä & Hendry, 2014). The main point in this paper is that disentanglement of these separate effects requires that the environmental zero-point u_{ref} is defined, and that this should not be done arbitrarily. Instead, it should be based on the environment u_0 where the phenotypic variance is at a minimum (Definition 1 and Fig. 1). This definition can be extended to multivariate cases. As shown in a toy example, large errors in u_{ref} may lead to large errors in predicted microevolutionary changes over time (Table 1 and Fig. 5). Such large errors in u_{ref} may occur when the range of environmental data used for predictions is far from the mean value of the stochastic environment the population is adapted to.

Although the plastic response to climate change is a result of individual plasticity, it should be noted that individual traits do not enter into the prediction equations (6a,b), but instead the individual phenotypic and fitness values (Fig. 4). Similarly, individual traits do not determine the environmental value u_0 in Definition 1, but instead the phenotypic variance (Fig. 1).

In theoretical studies it is often assumed that the environmental variable is scaled such that $u_{ref} = u_0 = 0$ (Lande, 2009; Chevin & Lande, 2015). This can be done also in databased applications, provided that u_0 is known, and that the correction term in Definition 1 is zero.

The toy example used in the simulations is a simplification of reality, because changing spring temperatures affect fitness in a complex way (Bowers et al., 2016). It still suffices to show that the environmental zero-point together with initial mean trait and parameter values can be estimated from environmental, phenotypic and fitness data, by use of the prediction error minimization method in Fig. 2. The simulations make use of an environmental trend, as in noisy temperature trends caused by climate change (Fig. 3), and a correct environmental zero-point then results in quite good predictions of changes in mean quantitative traits over time (Table 1, Case 1). Although these predictions are based on parameter estimation, all the separate parameter estimates as such are not especially good, although they were considerably improved when the population size was increased from 100 to $10{,}000$ (Appendix 3). The environmental zero-point can also be estimated, but with large standard errors, especially for small population sizes, and this results in a correspondingly large standard error in predicted change in mean intercept $\bar{a}_t$ over time (Table 1, Case 2). An estimated zero-point may still be a better choice than use of an initial environmental value in a recorded time series, or the mean value, which may give large errors in predicted changes in mean quantitative traits (Table 1, Case 3). Another alternative may be to use the mean value of a past stationary stochastic environment, which the population is judged to have been fully adapted to.

It is here assumed that the genetic relationship matrix is an identity matrix, and the simulation results are obtained by use of a prediction error minimization method. However, the fact that errors in the environmental zero-point may cause large errors in predictions of microevolution, as discussed in Subsection 2.5, is a generic problem. Independent of prediction method and the complexity of the model, an error in the environmental zero-point implies that an erroneous model is fitted to the input-output data, and that must inevitably result in prediction errors. An alternative view when $\hat{u}_{ref} \neq u_{ref}$ is constant (Case 3), is that the tuning model in Fig. 2 still uses the correct value of u_{ref}, but then with an error term $u_{ref} - \hat{u}_{ref}$ added to the environmental input. In order to minimize $\sum_{t=1}^{T}(\bar{y}_t - \hat{\bar{y}}_t)^2$, this input error must as good as possible be compensated by errors in estimated parameter values, resulting in prediction errors. Note that this argument is independent of the specific parametrizations used in the microevolutionary and tuning models in Fig. 2. It is in any case no reason to believe that prediction errors caused by $\hat{u}_{ref} \neq u_{ref}$ will disappear in cases where the genetic relationship matrix is not a unity matrix, and when other parameter estimation and mean trait prediction methods are used. A more specific argument regarding BLUP/REML parameter estimation is given in Appendix 4. It must thus be expected that predictions of microevolutionary changes over time depend on the chosen environmental zero-point (reference environment), and such predictions cannot therefore be trusted unless the chosen environmental zero-point can be trusted. Exceptions are here cases with a constant mean plasticity slope, where the change in mean reaction norm intercept per generation according to Equation (5) is independent of the environmental zero-point. This implies that a nearly constant mean plasticity slope must be expected to result in small errors in the predicted changes of the mean intercept, also if there is an error in the environmental zero-point.

Acknowledgement

The derivation of prediction equations in Appendix 1 was inspired by a review comment by Michael Morrissey, although on a quite different manuscript with a derivation directly based on the Price equation. I thank University of South-Eastern Norway for support and funding.

Author Contribution

Rolf Ergon is the sole author of this article.

Data Accessibility Statement

MATLAB code for simulations is given in Supplementary Material archived in *biorxiv*.

Conflict of interest

The author declares no conflict of interest.

References

Chevin, L.-M., & Lande, R. (2015). Evolution of environmental cues for phenotypic plasticity. Evolution, 46(2), 390–411. doi:10.1111/evo.12755

Bowers, E.K., Grindstaff, J.L., Soukup, S.S., Drilling, N.E., Eckerle, K.P., Sakaluk, S.K., & Thompson, C.F. (2016). Spring temperatures influence selection on breeding date and the potential for phenological mismatch in a migratory bird. Ecology, 97(10), 2880–2891.

Ergon, T., & Ergon, R. (2017). When three traits make a line: evolution of phenotypic plasticity and genetic assimilation through linear reaction norms in stochastic environments. J. Evol. Biol. 30, 486-500. doi: 10.1111/jeb.13003

Ergon, R. (2018). The environmental zero-point problem in evolutionary reaction norm modeling. Ecol Evol. 8, 4031–4041. doi: 10.1002/ece3.3929

Fossen, E.I.F., Pélabon, C. & Einum, S. (2018). An empirical test for a zone of canalization in

thermal reaction norms J. Evol. Biol. 31, 936-943. doi: 10.1111/jeb.13287.

Lande, R. (1979). Quantitative genetic analysis of multivariate evolution, applied to brain:body size allometry. Evolution 33, 402-416.

Lande, R. (2009). Adaptation to an extraordinary environment by evolution of phenotypic plasticity and genetic assimilation. J. Evol. Biol. 22, 1435-1446. doi: 10.1111/j.1420-9101.2009.01754.x

Ljung, L. (2002). Prediction Error Estimation Methods. Circuits, Systems, and Signal Processing 21/1, 11-21.

Lynch, M., & Walsh, B. (1998). Genetics and Analysis of Quantitatve Traits. Sinauer Associates, Mass.

Merilä, J., & Hendry, A.P. (2013). Climate change, adaptation, and phenotypic plasticity: the problem and the evidence. Evol. Appl. 7, 1-14. doi: 10.1111/eva. 12137.

Morrissey, M.B., Kruuk, L.E.B, & Wilson, A.J. (2010) The danger of applying the breeder's equation in observational studies of natural populations. J. Evol. Biol. 23, 2277-2288. doi: 0.1111/j.1420-9101.2010.02084.x

Appendix 1. Derivation of prediction equations

The goal is to find Equations (6a,b) for incremental changes $\Delta\bar{a}_t = \bar{a}_{t+1} - \bar{a}_t$, $\Delta\bar{b}_t = \bar{b}_{t+1} - \bar{b}_t$, and thus also $\Delta\bar{y}_t = \bar{y}_{t+1} - \bar{y}_t$, by means of a common selection gradient $\beta_{y,t}$. Note that these equations implicitly assume that the additive genetic relationship matrix $\boldsymbol{A}_t$ in Fig. 2 is a unity matrix, if not the genetic relationships will simply be ignored.

As stated in the main text, a fundamental equation for mean trait predictions follows from Equation (2a) as

$$\Delta\bar{y}_t = \Delta\bar{a}_t + \Delta\bar{b}_t\left(u_{t+1} - u_{ref}\right) + \bar{b}_t\Delta u_t, \tag{5}$$

where $\Delta u_t = u_{t+1} - u_t$. From this follows that the value of u_{ref} has nothing to say in special cases with constant mean plasticity slopes, i.e., when $\Delta\bar{b}_t = 0$. In such cases we simply have $\Delta\bar{y}_t = \Delta\bar{a}_t + \bar{b}\Delta u_t$, where $\bar{b}$ is constant, or only $\Delta\bar{y}_t = \bar{b}\Delta u_t$ if $\bar{a}_t$ does not evolve.

In the general case, $\Delta\bar{a}_t$ and $\Delta\bar{b}_t$ are found from Equations (6a,b), as derived below. Assuming a constant environment, i.e., for $\Delta u_t = 0$, Equation (5) gives $\Delta\bar{y}_t^c = \Delta\bar{a}_t + \Delta\bar{b}_t\left(u_{t+1} - u_{ref}\right)$, which by means of the breeder's equation (Lande, 1979) also can be written as

$$\Delta\bar{y}_t^c = G_{yy,t}^c\beta_{y,t} = G_{yy,t}^c\frac{1}{\bar{W}_t}\,P_{yy,t}^{-1}cov\left(W_{i,t}, y_{i,t}\right), \tag{A1}$$

where $\beta_{y,t}$ is the selection gradient, while $G_{yy,t}^c$ and $P_{yy,t}$ are additive genetic and phenotypic variances, respectively. Here, $W_{i,t}$ is the individual fitness, with population mean value $\bar{W}_t$, while $y_{i,t}$ is the individual phenotypic value. We must assume that values of $W_{i,t}$ and $y_{i,t}$ are available.

In order to find expressions for $\Delta\bar{y}_t$, $\Delta\bar{a}_t$ and $\Delta\bar{b}_t$, we may express $\Delta\bar{a}_t$ and $\Delta\bar{b}_t$ by means of $\beta_{y,t}$ according to

$$\begin{bmatrix} \Delta\bar{a}_t \\ \Delta\bar{b}_t \\ \Delta\bar{y}_t^c \end{bmatrix} = \boldsymbol{G}_{aby,t} \begin{bmatrix} 0 \\ 0 \\ \beta_{y,t} \end{bmatrix}, \tag{A2}$$

where the $\boldsymbol{G}_{aby,t}$ matrix is found via the linear transformation of the vector $[a_{i,t} \quad b_{i,t}]^T$ onto the vector $[a_{i,t} \quad b_{i,t} \quad y_{i,t}]^T$. By use of Equation (1) we find (using $u_t' = u_t - u_{ref}$)

$$\begin{bmatrix} a_{i,t} \\ b_{i,t} \\ y_{i,t} \end{bmatrix} = \begin{bmatrix} 1 & 0 \\ 0 & 1 \\ 1 & u_t' \end{bmatrix} \begin{bmatrix} a_{i,t} \\ b_{i,t} \end{bmatrix} + \begin{bmatrix} 0 \\ 0 \\ v_{i,t} + \eta_{i,t} u_t' \end{bmatrix}, \tag{A3}$$

such that the additive genetic covariance matrix of $[a_{i,t} \quad b_{i,t} \quad y_{i,t}]^T$ specific to the environment u_t' becomes

$$\boldsymbol{G}_{aby,t}(u_t') = \begin{bmatrix} 1 & 0 \\ 0 & 1 \\ 1 & u_t' \end{bmatrix} \begin{bmatrix} G_{aa} & G_{ab} \\ G_{ab} & G_{bb} \end{bmatrix} \begin{bmatrix} 1 & 0 & 1 \\ 0 & 1 & u_t' \end{bmatrix}$$

$$= \begin{bmatrix} G_{aa} & G_{ab} & G_{aa} + G_{ab} u_t' \\ G_{ab} & G_{bb} & G_{ab} + G_{bb} u_t' \\ G_{aa} + G_{ab} u_t' & G_{ab} + G_{bb} u_t' & G_{aa} + G_{ab} u_t' + G_{ab} u_t' + G_{bb} u_t'^2 \end{bmatrix}. \tag{A4}$$

From Equations (A1), (A3) and (A4) follow

$$\Delta\bar{a}_t = (G_{aa} + G_{ab} u_t') \frac{1}{\bar{W}_t} P_{yy,t}^{-1} cov\left(W_{i,t}, y_{i,t}\right), \tag{A5a}$$

and

$$\Delta\bar{b}_t = (G_{ab} + G_{bb} u_t') \frac{1}{\bar{W}_t} P_{yy,t}^{-1} cov\left(W_{i,t}, y_{i,t}\right). \tag{A5b}$$

where

$$P_{yy,t} = G_{aa} + \sigma_v^2 + 2G_{ab} u_t' + \left(G_{bb} + \sigma_\eta^2\right) u_t'^2. \tag{A5c}$$

Since only a single environmental value is involved in Equations (A5a,b), they are valid in any environment, also if it varies with time¸ and $\Delta\bar{y}_t$ thus follows by inserting $\Delta\bar{a}_t$ and $\Delta\bar{b}_t$

from Equations (5a,b) into Equation (5). For computations of $\bar{a}_t$ and $\bar{b}_t$, and thus $\bar{y}_t$, initial values of $\bar{b}_t$ and $\bar{b}_t$ are needed.

Alternatively, $\Delta\bar{y}_t$ is found as

$$\Delta\bar{y}_t = (G_{aa} + G_{ab}u'_t + G_{ab}u'_{t+1} + G_{bb}u'_t u'_{t+1})\frac{1}{\bar{W}_t}P_{yy,t}^{-1}cov\left(W_{i,t}, y_{i,t}\right) + \bar{b}_t\Delta u_t. \quad \text{(A6)}$$

Note that $G_{yy,t}^{c}$ in Equation (A1) follows from $G_{yy,t}$ according to Equation (A6) by setting $u'_{t+1} = u'_t$, i.e., under the assumption of a constant environment. The same expression for $G_{yy,t}^{c}$ also follows from Equation (A4).

Appendix 2. Modeling error results

Simulations with a true three-trait reaction norm model according to Equation (8), i.e., with a perception trait in addition to the intercept and plasticity traits (Ergon & Ergon, 2017), but with a two-trait prediction model, gave increased prediction errors as compared to results in Table 1. The population size was $N = 100$. Simulations with $G_{cc} = G_{aa} = 0.025$ and the true value $u_{ref} = 0$, gave the following results: With $G_{ac} = 0$ the prediction errors were $\Delta_{30}^{error}\hat{\bar{a}}_t\% = -14 \pm 8$ and $\Delta_{30}^{error}\hat{\bar{b}}_t\% = 2 \pm 7$. With $G_{ac} = -0.01$ the results were $\Delta_{30}^{error}\hat{\bar{a}}_t\% = -39 \pm 7$ and $\Delta_{30}^{error}\hat{b}_t\% = -2 \pm 4$, while $G_{ac} = 0.01$ gave $\Delta_{30}^{error}\hat{\bar{a}}_t\% = 9 \pm 8$ and $\Delta_{30}^{error}\hat{\bar{b}}_t\% = 0 \pm 5$. Note that $\Delta_{30}^{error}\hat{b}_t\%$ is very much the same for all values of G_{ac}.

Typical responses are shown in Fig. A1. Note especially that the change in $\bar{a}_t$ over time for $G_{ac} \leq 0$ is underestimated, which indicates that modeling errors in general may result in underestimated changes in $\bar{a}_t$. This should be compared with the results for Case 3 in Table 1, where changes in $\bar{a}_t$ are overestimated.

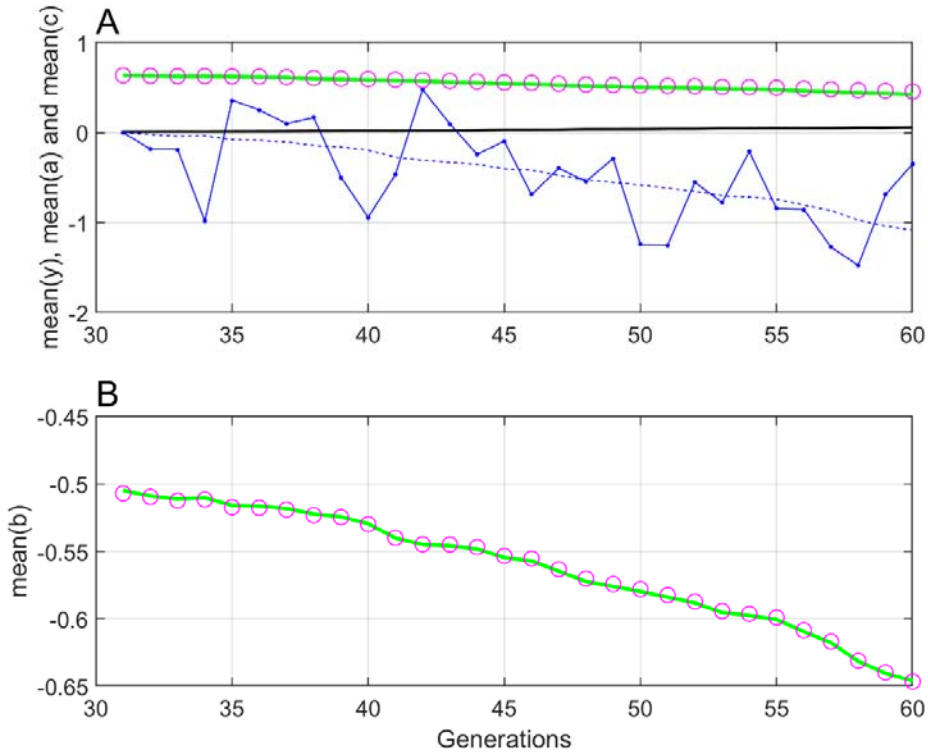

Figure A1. Typical responses as for Case 1 in Fig. 5, but with a true three-trait model according to Equation (8) with $G_{cc} = G_{aa} = 0.025$ and $G_{ac} = 0$. The true $\bar{c}_t$ response is shown by black line.

Appendix 3. Results with increased population size

Table A1 shows results as in Table 1, but with population size $N = 10{,}000$.

Table A1. Estimation and prediction results as in Table 1, but with population size $N = 10{,}000$. In Case 3, 16% of the simulations were discarded because $\sum \varepsilon_{t,final}^2 > 0.001$.

Parameter etc.	True value	Optimization results Case 1	Optimization results Case 2	Optimization results Case 3
$\hat{G}_{bb}$	0.01	0.0100 ± 0.0003	0.0103 ± 0.0023	0.0064 ± 0.0017
$\hat{G}_{ab}$	0	0.0006 ± 0.0033	0.0002 ± 0.0029	0.0068 ± 0.0015
$\hat{\sigma}_v^2$	0.025	0.0269 ± 0.0064	0.0277 ± 0.0146	0.0256 ± 0.0034
$\hat{\sigma}_\eta^2$	0.01	0.0103 ± 0.0021	0.0102 ± 0.0026	0.0161 ± 0.0027
$\hat{\hat{b}}_{31}$	–	-0.4958 ± 0.0068	-0.4962 ± 0.0086	-0.4969 ± 0.0089
$\hat{u}_{ref}$	10	10	9.9483 ± 0.1921	11
$\sum \varepsilon_{t,final}^2$	–	$10^{-5}(0 \pm 2)$	$10^{-5}(1 \pm 2)$	$10^{-5}(10 \pm 10)$
$\Delta_{30}^{error} \hat{a}_t \%$	–	0 ± 1	-3 ± 12	68 ± 6
$\Delta_{30}^{error} \hat{\hat{b}}_t \%$	–	0 ± 1	0 ± 1	-4 ± 3
$\Delta_{30,corr}^{error} \hat{\hat{a}}_t \%$	–	0 ± 1	0 ± 1	4 ± 4

Appendix 4. REML parameter estimation

The reaction norm model in Equation (1) can by use of Equation (2a) be written as

$$y_{i,t} = \bar{y}_t + a_{i,t} - \bar{a}_t + \left(b_{i,t} - \bar{b}_t\right)(u_t - u_{ref}) + v_{i,t} + \eta_{i,t}(u_t - u_{ref}). \tag{A7a}$$

From this follows the random mixed model for the population,

$$\boldsymbol{y}_t = \boldsymbol{1}_N \bar{y}_t \; + [\boldsymbol{I}_N \quad \boldsymbol{U}_t] \begin{bmatrix} \boldsymbol{a}'_t \\ \boldsymbol{b}'_t \end{bmatrix} + [\boldsymbol{I}_N \quad \boldsymbol{U}_t] \begin{bmatrix} \boldsymbol{v}_t \\ \boldsymbol{\eta}_t \end{bmatrix}, \tag{A7b}$$

where $\boldsymbol{a}'_t = \boldsymbol{a}_t - \boldsymbol{1}_N \bar{a}_t$ and $\boldsymbol{b}'_t = \boldsymbol{b}_t - \boldsymbol{1}_N \bar{b}_t$, where $\boldsymbol{1}_N$ is an $N \times 1$ vector of ones. Here, $\boldsymbol{y}_t$, $\boldsymbol{a}_t$, $\boldsymbol{b}_t$ $\boldsymbol{a}'_t$, $\boldsymbol{b}'_t$, $\boldsymbol{v}_t$ and $\boldsymbol{\eta}_t$ are $N \times 1$ vectors of individual values at time t, while $\bar{y}_t$ is the scalar valued fixed effect. The environmental input is $\boldsymbol{U}_t = (u_t - u_{ref})\boldsymbol{I}_N$, where $\boldsymbol{I}_N$ is the $N \times N$ unity matrix. The expected values $E[\boldsymbol{a}'_t]$, $E[\boldsymbol{b}'_t]$, $E[\boldsymbol{v}_t]$ and $E[\boldsymbol{\eta}_t]$ are all zero by definition (Ch. 26, Lynch and Walsh, 1998).

The starting point for REML parameter estimation based on the model (A7b) is the phenotypic population covariance matrix $\boldsymbol{V}_t = E[(\boldsymbol{y}_t - \boldsymbol{1}_N \bar{y}_t)(\boldsymbol{y}_t - \boldsymbol{1}_N \bar{y}_t)^T]$ (Ch. 27, Lynch and Walsh, 1998). For the model in Equation (1) this covariance matrix is

$$\begin{aligned} \boldsymbol{V}_t &= E\left[\left(\boldsymbol{a}_t - \boldsymbol{1}_N \bar{a}_t + \boldsymbol{v}_t + \left(\boldsymbol{b}_t - \boldsymbol{1}_N \bar{b}_t\right)\left(u_t - u_{ref}\right) + \boldsymbol{w}_t\left(u_t - u_{ref}\right)\right)(\cdot)^T\right] \\ &= \left(G_{aa} + 2G_{ab}\left(u_t - u_{ref}\right) + G_{bb}(u_t - u_{ref})^2\right)\boldsymbol{A}_t + \left(\sigma_v^2 + (u_t - u_{ref})^2 \sigma_\eta^2\right)\boldsymbol{I}_N, \end{aligned} \tag{A8}$$

where $\boldsymbol{A}_t$ is the genetic relationship matrix (Ch. 27, Lynch and Walsh, 1998). From Equation (A8) follows that REML parameter estimation results depend on u_{ref}, such that errors in the environmental zero-point give errors in estimated parameter values. As in parameter estimation based on Equations (6a,b), we can in REML estimation set G_{aa} to any value, and estimate other parameters in relation to that. It follows from Equation (A8) that we cannot find $\hat{G}_{ab}$ separate from $\hat{G}_{bb}$, and $\hat{\sigma}_v^2$ separate from $\hat{\sigma}_\eta^2$, unless data for several different values of u_t are used. This may be compared with the PEM method in Fig. 2, as used in the simulations, where data from all available generations are utilized.